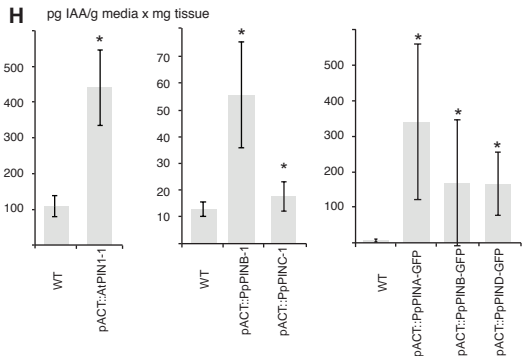
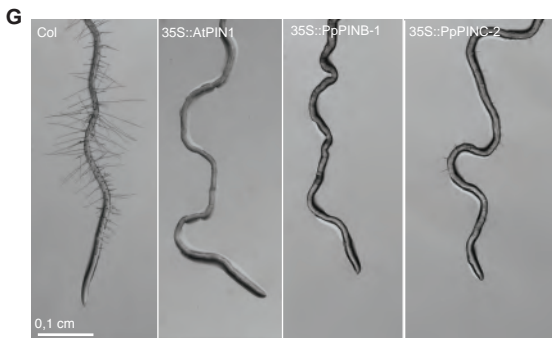
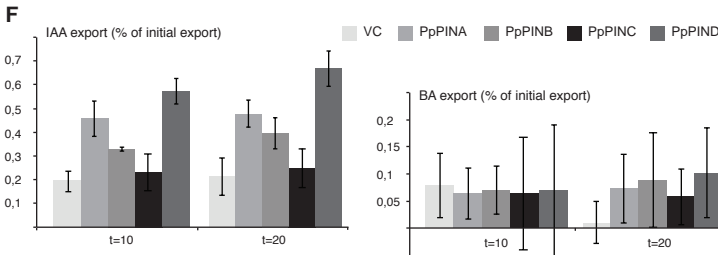
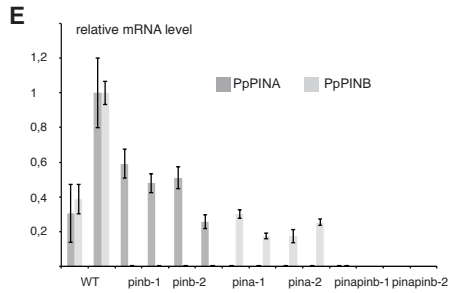
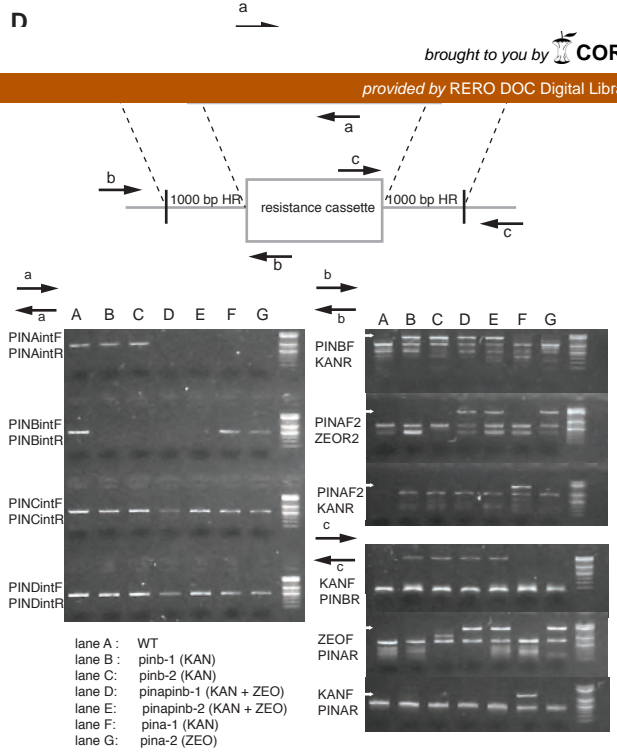
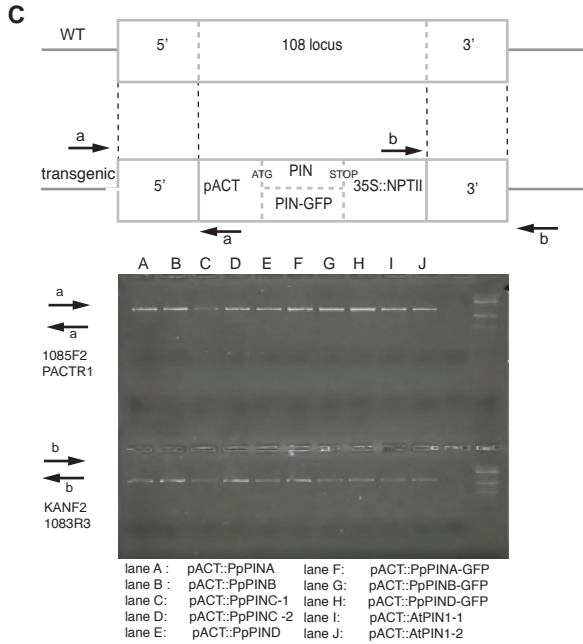
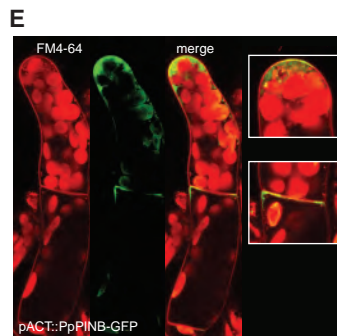
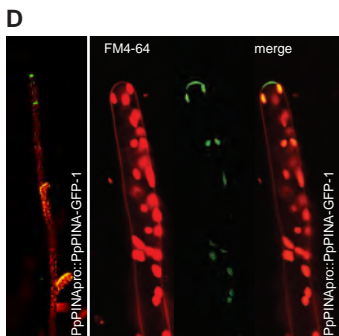
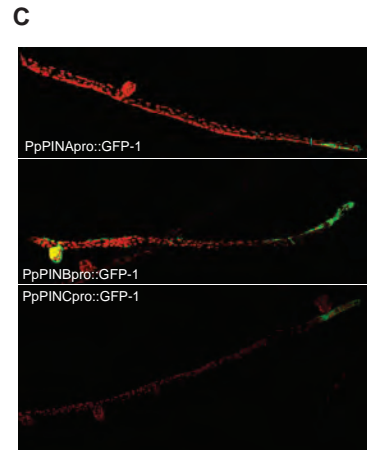
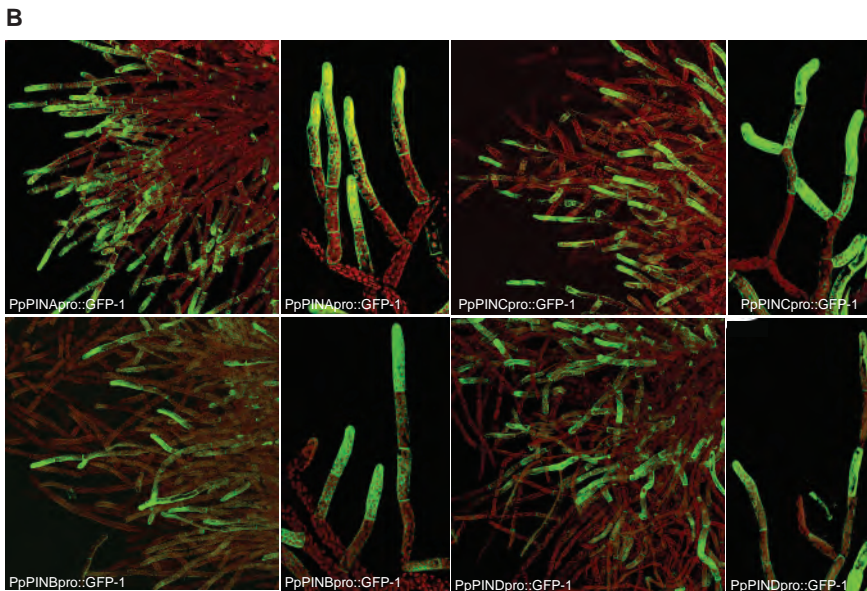
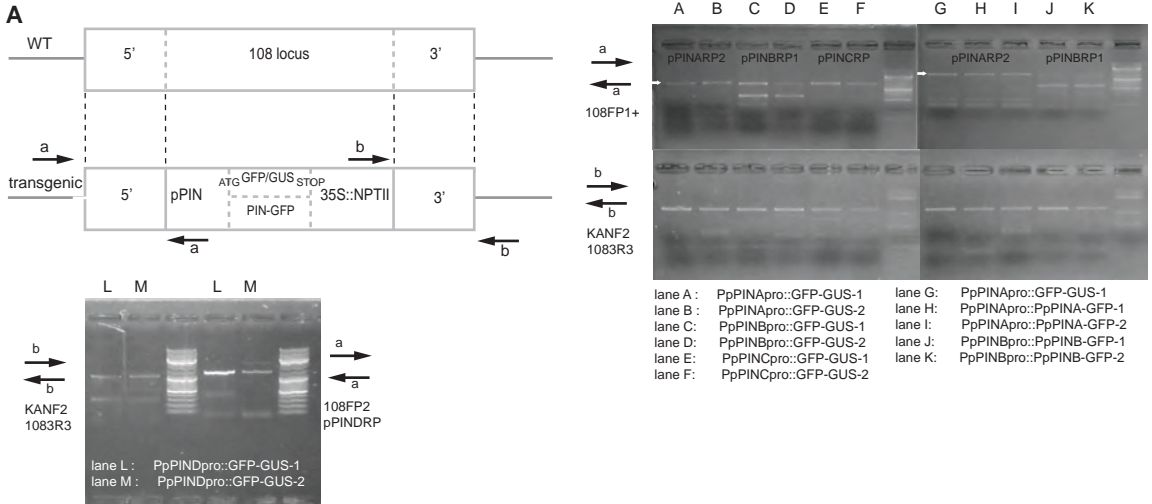


B

PpPINA AKKSMPPSAVM 552 GFP IKLIAVMTFRKLVVNPNTYS
 PpPINB AKKSMPPSAVM 552 GFP IKLIAVMTFRKLVVNPNTYS
 AtPIN1 QAKVMPPTSVM 461 GFP TRLLIMVVRKLRINPNYSYS
 PpPIND KEVRKMGQPAV 163 GFP GSVAGRNSFSVANGESGTR

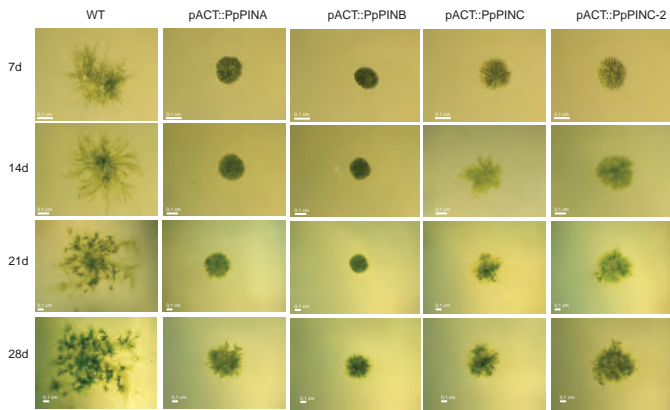


Suppl. Fig.2

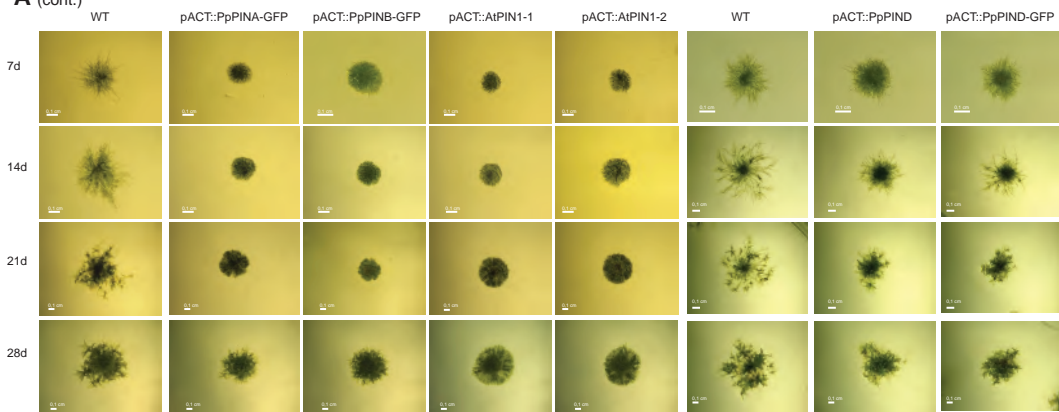


Suppl. Fig.3

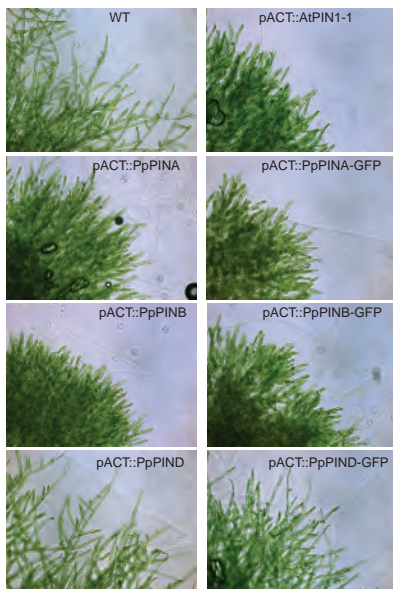
A



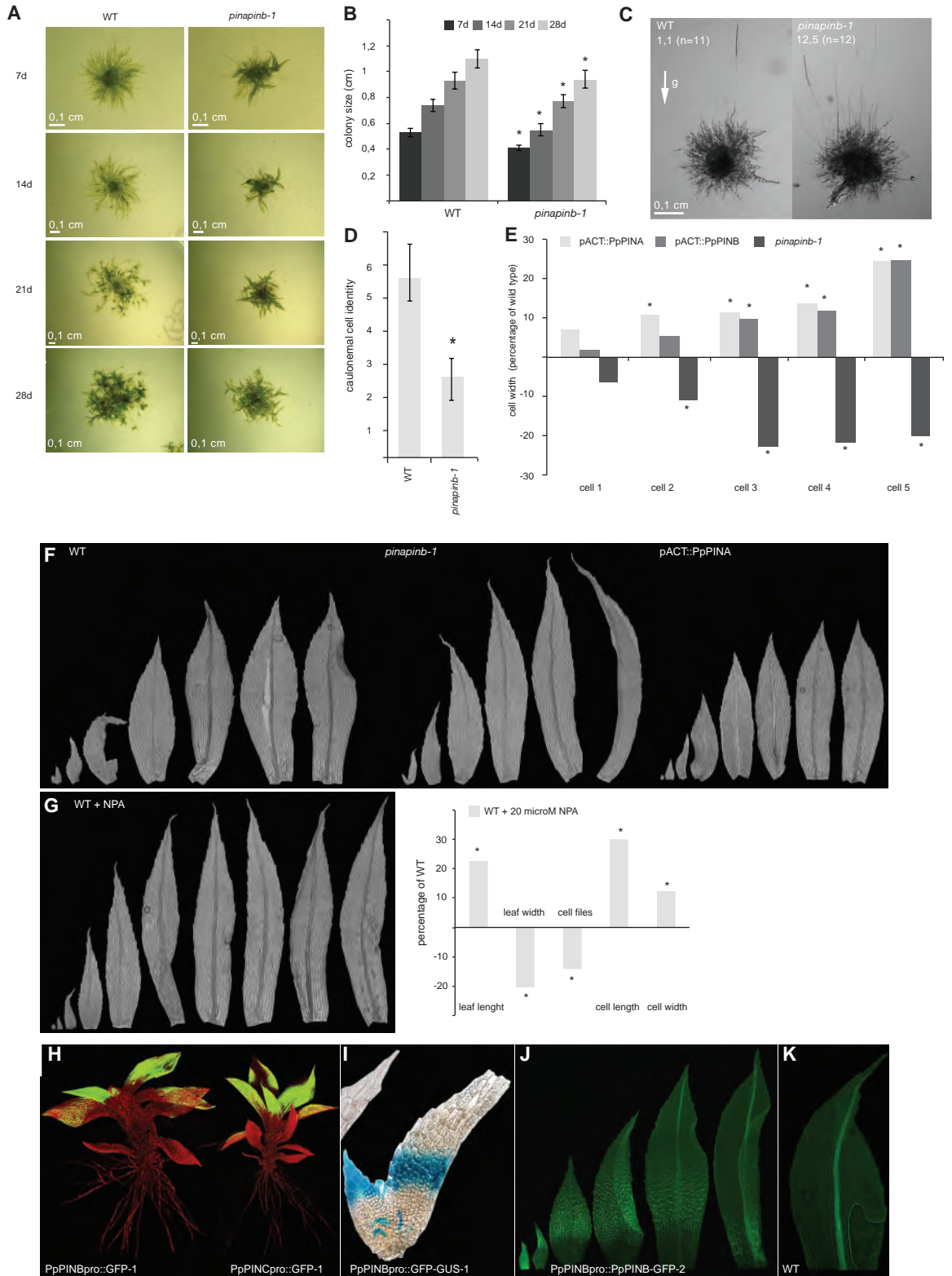
A (cont.)



B



Suppl. Fig.4



Figures S1-S4

Figure S1. Vector map, translational fusions to eGFP, generation of PIN OE and knockout lines in *P. patens*, auxin transport assays of PIN proteins in *N. benthamiana* protoplasts, *Arabidopsis* root hair assays and *P. patens* auxin export assays (supplement to Figure 1)

(A). Vector map of the gateway multisite destination vector pL5-m34GW7-K-L3 used to target the *P. patens* 108 silent locus by homologous recombination (36). (B). Protein alignment showing the position where eGFP was inserted to generate the translational fusions. The number indicates the amino acid position in the PIN protein sequence. (C). Principal construct overview and PCR confirmation of transgenic *P. patens* lines overexpressing different PIN proteins, with or without the eGFP-tag. (D). Principal construct overview and PCR confirmation of *P. patens* *PpPINA* and *PpPINB* single and double KO lines. (E). qPCR showing transcriptional activity of *PpPINA* and *PpPINB* in WT, single and double KO lines. (F) Auxin transport assays in mesophyll protoplasts from transiently transfected *N. benthamiana* leaves indicate that PpPINs enhance export of IAA and not BA over time. Presented are average values of IAA and BA export measurements from at least 3 independent protoplast infiltrations at two different timepoints (in minutes). VC (empty silencing *Agrobacterium*) was used as control. (G). Overexpression of long PINs from both *Arabidopsis* (*AtPIN1*) and *P. patens* (*PpPINB* and *PpPINC*) strongly inhibits root hair development in *Arabidopsis*. Data are presented as mean \pm s.d. All primers used in this figure can be found in Table S1. (H). Transgenic *P. patens* lines overexpressing long PINs from

Arabidopsis (*AtPIN1*) and *P. patens* PpPINs (*PpPINB* and *PpPINC*; *PpPINA-GFP*, *PpPINBGFP* and *PpPIND-GFP*) enhance IAA export into the medium. Free IAA in liquid media per mg moss tissue is shown. Data are presented as mean \pm s.d.; * $P < 0.05$ (by Student's t-test).

Figure S2. Generation of *PpPIN* transcriptional and translational fusions and expression and localization of PIN proteins during protonemal development (supplement to Figure 2)

(A). Principal construct overview and PCR confirmation of transcriptional and translational reporter *P. patens* lines under endogenous *PpPIN* promoters. All primers used in this figure can be found in Table S1. (B). Transcriptional reporter lines show activity of the long *PpPINA-D* genes during *P. patens* chloronemal development. Expression of long *PpPINA-C* gradually increases towards the tip of the chloronemal filaments. Transcriptional reporter line of the short *PpPIND* proteins shows a less pronounced graded expression in chloronemal filaments. (C). Transcriptional reporter lines show activity of the long PpPIN genes during *P. patens* caulonemal development. *PpPINA-C* and promoters show an increasing activity towards the tip in caulonemal filaments. (D). The PpPINA-GFP-1 fusion protein expressed by PpPINAs native promoter co-localizes with the fluorescent PM-marker FM4-64 at the apical membrane of the tip cell in a caulonemal filament. (E) Overexpression of translational fusion of the long PpPINB to GFP shows co-localization with FM4-64 at the distal cell side towards the filament tip. All pictures are taken using a Carl Zeiss LSM 710 confocal microscope. Autofluorescence of chloroplasts is obvious in both the green and red channel.

Figure S3. Overexpression of long and short PpPINs (with and without eGFP) and *AtPIN1* in

P. patens (supplement to Figure 3)

(A). *P. patens* colonies of all different OE genotypes (with and without eGFP) and WT were followed over time during four weeks. Pictures were taken with a binocular microscope. In general, long PpPIN OE (with and without the eGFP tag) and AtPIN1 OE lines show a significant reduced colony proliferation compared to WT. Colony growth of the short PpPIND OE line (with and without tag) is very similar to WT and only slightly reduced in size. While OE of long PpPIN (with and without tag) and AtPIN1 delays the appearance of gametophores, OE of short PpPIND (with and without tag) does not change the timing and amount of gametophores on the colonies. Numerical data can be found in Table S2 (B). Detailed pictures of colony edges of selected OE genotypes; OE of long PpPIN (with and without tag) and AtPIN1 reduces the growth of protruding caulonemal filaments, while OE of short PpPIND (with and without tag) behaves like WT.

Figure S4. Detailed analyses of protonemal development in *pinapinb* KO and PIN OE lines, expression and localization of long PpPINs during gametophore development and detailed analyses of gametophore development in *pinapinb* KO and PIN OE lines (supplement to Figure 3 and 4)

(A). Colonies of *pinapinb* KO and WT followed during four weeks. (B). The *pinapinb* mutant line produces consistently smaller colonies. (C). Dark-grown colonies of a dKO line produce more caulonemal filaments than WT in the same timeframe. Numbers indicate the average number of caulonemal filaments growing out from the colony. The white arrow indicates the

gravity vector. **(D)**. Regenerating chloronemal filaments from protoplasts show an earlier transition to caulonemal cell identity in a *pinapinb* mutant line. Data is presented as the first cell in the regenerating filament that shows caulonemal cell identity. Data are represented as mean \pm s.d.; * $P < 0.05$ (by Student's t-test). **(E)**. OE and dKO of long PIN proteins have an opposite effect on the cell width in regenerating protonemal filaments. While OE increases, dKO of long PIN proteins reduces cell width significantly. **(F)**. Leaf developmental series of WT (leaf P1-P8), *pinapinb* mutant (leaf P2-P8) and PpPINA OE lines (leaf P1-P8) show altered leaf development. *Pinapinb* mutant leaves are narrower and longer, while PpPINA OE leaves are narrower and shorter compared to WT leaves. **(G)**. Leaf developmental series of WT colonies grown on 20 microM NPA (leaf P1-P10) show altered leaf development, with narrower and longer leaves, similar to *pinapinb* dKO lines. They also have a reduced number of cell files, pointing towards a reduced cell division. Cells in the leaves are longer and wider, suggesting stimulated elongation of cells, when treated with 20 microM NPA. Data is presented as the percentage of increase or decrease compared to WT. Data are represented as mean \pm s.d.; * $P < 0.05$ (by Student's t-test). **(H)**. The *PpPINC* and *PpPINB* promoters are highly active in developing leaves of the gametophytic shoots. **(I)**. GUS staining in leaves of *PpPINB* transcriptional reporter line reveals a strong *PpPIN* expression domain at the tip of young leaves that gradually moves towards the base of the leaves as well as expression in the axillary hairs. **(J)**. Translational reporter line of *PpPINB* shows a basipetal wave of PIN expression during leaf development (from leaf P3 to leaf P8). **(K)**. WT leaf showing strong autofluorescence in the midrib cells of fully developed leaves.

Table S1. Overview of primers used in this paper.

Table S2. Detailed comparison of developmental phenotypes and transgene expression of different genotypes expressing PIN proteins, with or without tag, under the actin promoter.

(A-B) Colony size (in square mm) and number of gametophores is followed during four weeks of growth. In general, long PpPIN OE (A-C, with and without the eGFP tag) and AtPIN1 OE lines show a significant reduced colony proliferation compared to WT. Colony growth of the short PpPIND OE line (with and without tag) is very similar to WT and only slightly reduced in size. While OE of long PpPIN (with and without tag) and AtPIN1 delays the appearance and decreases the total amount of gametophores, OE of short PpPIND (with and without tag) does not change the timing and amount of gametophores on the colonies. Data are presented as mean with s.d. in between brackets. Number is highlighted when significantly different from WT ($p < 0.005$, t-test). **(C)** Relative transgene expression by qPCR (both PIN and resistance cassette) is shown in the *P. patens* OE lines.

Supplementary Table 1

KNOCKOUT

pDONR P4-P1R	PINAHRattB4F	GGGGACAACCTTTGTATAGAAAAGTTGCCCTGTATCCTGTTCCACTGCG
	PINAHRattB1R	GGGGACTGCTTTTTTTGTACAAAAGCTTTGAGAACGTTTGCCGGC
	PINBHRattB4F	GGGGACAACCTTTGTATAGAAAAGTTGCCATATGTTGGGTGCGTCATTCT
	PINBHRattB1R	GGGGACTGCTTTTTTTGTACAAAAGCTTTGACAGAGGTTAAGTACTG
pDONR221	ZeoattB1F	GGGGACAAGTTTGTACAAAAAGCAGGCTCCCTTTTCAGAAAAGATGCTAACCC
	ZeoattB2R	GGGGACCCTTTGTACAAAAGAAAGCTGGGTCCCGTACCCGGTGTGAGGGA
	KanattB1F	GGGGACAAGTTTGTACAAAAAGCAGGCTCCCCATGGAGTCAAAGATTCAAAT
	KanattB2R	GGGGACCCTTTGTACAAAAGAAAGCTGGGTTCATTCGAGCTCGGTACCCCTG
pDONR P2R-P3	PINAattB2F	GGGGACAGCTTTCTTGTACAAAAGTGGCCCTGGCTGGCAAGTGTATTTT
	PINAattB3R	GGGGACAACCTTTGTATAATAAAAGTTGCAAACTGGCCATGTCCGGTCAA
	PINBattB2F	GGGGACAGCTTTCTTGTACAAAAGTGGCCCGTACTGGAAAATGCCGCTTT
	PINBattB3R	GGGGACAACCTTTGTATAATAAAAGTTGCTTACCGAACATTGCGAGCATG
AMPLIFICATION	PINAKOF	TGTATCCTGTTCCACTGCG
	PINAKOR	AAACTGGCCATGTCCGGTCAA
	PINBKOF	ATATGTTGGGTGCGTCATTCT
	PINBKOR	TTACCGAACATTGCGAGCATG
GENOTYPING	PINAintF	GCCTCCCACTTGCATGAATA
	PINAintR	ATTGTGGAAAACCCATGCTC
	PINBintF	CATCTCCACAGGAGTTCGT
	PINBintR	TCAGTTGGTGATGGCAAGAA
	PINCintF	GGCCTCTCTGAACAAAGCTG
	PINCintR	CGAATTTTAAATGCTCTTATGTTGAA
	PINDintF	TCCCTGTCTGTTTCGACTACAA
	PINDintR	ATTCACGCAGGCTCAAAAAGT
	PINAF2	CTGTGCATTTGCTGTGAGGT
	ZEOR2	GGGGCTTATGCGGATTATTT
	ZEOF	GAACTCGCCGTAAGACTGG
	PINAR	GAATGTGCTAGCAGGCGATT
	KANR	CATGGGTACGACGAGATCCT
	PINBF	ATATGTTGGGTGCGTCATTCT
	KANF	TCGCCTTCTTGACGAGTCT
	PINBR	CCAAAGCAAACCAGTCAACA
	PINAF2	CTGTGCATTTGCTGTGAGGT
	KANR	CATGGGTACGACGAGATCCT
	KANF	TCGCCTTCTTGACGAGTCT

qPCR

PpPINAfpqPCR	AGTGCGCATGCTTGTACATC
PpPINARpqPCR	CCAAAGCTGAAGTCTCTCG
PINBqPCRfb	GTTGCAATAGGTGGCATTTC
PINBqPCRrb	ATCCCAAGTCCTGCATCTGA
ACT3qPCRfb	GAATGGTCAAGGCTGGTTTC
ACT3qPCRrb	TACCGACCATCACACCAGT
PpL21FqPCR	GTACTCGAGAAGCCAGACTTCCTAC
PpL21RqPCR	TCAATCTTCTTAGCATCACGGTACT
PpPINCfpqPCR	AGAAGTGGCTATGCTTGTGC
PpPINCrpqPCR	AAGTTCTGGGGTTCGCTTCT
PpPINDfpqPCR	ACCGCCTAATTGCTGCATAC
PpPINDrpqPCR	CACAATCCAACGAGAACGATT
KANF	ATCCATCATGGCTGATGCAATGCC
KANR	GATGTTTCGCTTGGTGGTCAAT
PIN1-Fw	TACTCCGAGACCTTCCAACCTA
PIN1-Rv	TCCACCGCCACCCTTCC
QEIF4A_FW	ACGGAGACATGGACCAGAAC
QEIF4A_REV	GCTGAGTTGGGAGATCGAAG

OVEREXPRESSION

pDONR P4-P1R	proACT1attB4F	GGGGACAACCTTTGTATAGAAAAGTTGTTTCGAGGTCATTTCATATGCTTG
	proACT1attB1rR	GGGGACTGCTTTTTTTGTACAAAAGCTTTGATATCCTCGGCGTCAGC
pDONR221	ATTB1PPPINAfP	GGGGACAAGTTTGTACAAAAAGCAGGCTTTATGATTAACGGCCATGACATA
	ATTB2PpPINAstopRP	GGGGACCCTTTGTACAAAAGAAAGCTGGGTTtcacagaccaagtaaatgta
	ATTB1PPPINBfP	GGGGACAAGTTTGTACAAAAAGCAGGCTTTATGATTAACGGCCATGACATT
	ATTB2PpPINBstopRP	GGGGACCCTTTGTACAAAAGAAAGCTGGGTTtcacagaccaagtaaatgta
	ATB1PPPINCfP2	GGGGACAAGTTTGTACAAAAAGCAGGCTTTATGATTAACGGGTCATGACATG
	ATTB2PpPINCstopRP	GGGGACCCTTTGTACAAAAGAAAGCTGGGTTtcagagcccagtaggatgta
	ATTB1PPPINDfP	GGGGACAAGTTTGTACAAAAAGCAGGCTTTATGTTGACAGGTGGTTCAGTTT
	ATTB2PpPINDstopRP	GGGGACCCTTTGTACAAAAGAAAGCTGGGTTtcagagttcaagtagttagta
	attB1fPIN1F	GGGGACAAGTTTGTACAAAAAGCAGGCTCCATGATTACGGCGGCGGACTT
	attB2RPIN1R	GGGGACCCTTTGTACAAAAGAAAGCTGGGTTTCATAGACCCAAGAGAATGTAG
GENOTYPING	Pp5locus108FP2	TCAACCTTGTATTACATCCACGA
	pACTgenotRP1	TCACTTGGGCCACCTTTTA
	KANcassforwardgenotyp2	GCGCGGTGTCATCTATGTTA
	108locus3Rgenotyp3	TCATCCATCCTTTCTTCATGC
	35SgenotypR	CTTTCTCTGTGTTCTTGATGCAG

TRANSCR./TRANSL. FUSIONS

pDONR P4-PIR

PpPINApromFP GGGGACAACCTTTGTATAGAAAAGTTGTTTCGCAGAATCTGTGCGCTTTCC
PpPINApromRP GGGGACTGCTTTTTTTGTACAAACTTGTGTTTGAGAACGTTTGTCCGGCC
PpPINBpromFP GGGGACAACCTTTGTATAGAAAAGTTGTTTGGATAATCGTAACTATAATA
PpPINBpromRP GGGGACTGCTTTTTTTGTACAAACTTGTGTTTGACAGAGGTTTAAAGTACT
PpPINCpromFP GGGGACAACCTTTGTATAGAAAAGTTGTTTCCTTTGTGTGGAGTAGAGTT
PpPINCpromRP GGGGACTGCTTTTTTTGTACAAACTTGTCTTGACGATCTGTGCGACGTGC
PpPINDpromFP GGGGACAACCTTTGTATAGAAAAGTTGTTGCGAGGACGGGGTTTCCTTC
PpPINDpromRP GGGGACTGCTTTTTTTGTACAAACTTGTGACGATAACGTTGATTGTCCT

overlapping PCR

PINARP1gfp2loop tcctcgcccttgctcaccatCATCACAGCAGAAGGTGGCA
PINAFP2gfp2loop gcatggacgagctgtacaagATTAAGCTAATTGCGGTCATG
GFPFPpina2loop TGCCACCTTCTGCTGTGATGatggtgagcaagggcgagga
GFPRPpina2loop CATGACCGCAATTAGCTTAAATctgtacagctcgtccatgc
PINBRP1gfp2 tcctcgcccttgctcaccatCATCACTGCCGAAGGTGGCA
PINBFP2gfp2 gcatggacgagctgtacaagATCAAGCTCATCGCTGTCATG
GFPFPpinb2 TGCCACCTTCGGCAGTGATGatggtgagcaagggcgagga
GFPRPpinb2 CATGACAGCGATGAGCTTGATctgtacagctcgtccatgc
PINDRP1gfp2 tcctcgcccttgctcaccatCACGGCAGGCTGACCCATTT
PINDFP2gfp2 gcatggacgagctgtacaagGGTTCGGTCGCACAACGAAA
GFPFPpind2 AAATGGGTCAGCCTGCCGTGatggtgagcaagggcgagga
GFPRPpind2 TTTCGTTGTGCGACGGAACCctgtacagctcgtccatgc

Supplementary Table 2

GENOTYPE	size (square mm)				# gametophores				relative transgene expression	
	1 WEEK	2 WEEKS	3 WEEKS	4 WEEKS	1 WEEK	2 WEEKS	3 WEEKS	4 WEEKS	PIN	nptII
WT	6,61 (0,56)	21,95 (2,85)	35,63 (4,62)	60,90 (8,23)	0,00	5,92 (1,34)	11,54 (1,76)	20,5 (3,30)		
pACT::PpPINA	5,42 (0,47)	10,86 (0,55)	20,91 (2,10)	37,96 (2,65)	0,00	0,17 (0,39)	3,23 (1,09)	17,42 (2,84)	1x	1x
pACT::PpPINA-gfp	3,98 (0,43)	6,82 (0,81)	11,21 (1,19)	20,51 (1,57)	0,00	0,00	1,43 (0,98)	9 (2,34)	6,8x	3,4x
pACT::PpPINB	2,89 (0,39)	4,10 (0,61)	7,91 (0,99)	16,97 (2,79)	0,00	0,08 (0,28)	0,46 (0,78)	6,17 (2,59)	1x	1x
pACT::PpPINB-gfp	3,50 (0,39)	6,17 (0,98)	12,94 (1,15)	28,30 (1,87)	0,00	1,08 (0,9)	5,75 (2,26)	14 (1,95)	2,2x	2,5x
pACT::PpPINC	5,26 (0,54)	10,95 (1,07)	18,39 (1,92)	33,64 (3,06)	0,00	3,1 (1,37)	7,82 (1,08)	14,73 (2,41)	1x	1x
pACT::PpPINC-2	5,90 (0,31)	12,75 (1,09)	24,15 (2,44)	44,37 (2,88)	0,00	1,6 (1,07)	8,3 (2,36)	18,8 (2,44)	1,1x	1,35x
WT	7,12 (1,55)	15,23 (1,55)	33,25 (3,92)	52,24 (8,39)	0,00	2,64 (1,50)	9,89 (2,32)	16,9 (2,92)		
pACT::PpPIND	4,79 (0,44)	13,39 (0,96)	21,84 (2,87)	41,32 (9,51)	0,00	2,45 (0,93)	8,5 (1,24)	15,09 (2,47)	1x	1x
pACT::PpPIND-gfp	5,11 (0,35)	15,37 (2,34)	20,87 (4,62)	36,77 (7,57)	0,00	4,25 (1,66)	11,33 (1,72)	17,58 (2,42)	4,9x	4,1x
WT	7,44 (1,05)	23,91 (2,77)	37,03 (4,62)	59,22 (7,34)	0,13 (0,35)	4,13 (1,46)	12,00 (2,58)	20,14 (2,73)		
pACT::AtPIN1-1	4,21 (0,78)	12,62 (2,17)	24,98 (3,39)	41,28 (5,04)	0,00	0,00	1,13 (1,13)	6,71 (3,45)	4,7x	1,4x
pACT::AtPIN1-2	3,95 (0,21)	9,72 (1,57)	18,74 (2,29)	30,36 (4,28)	0,00	0,00	1,13 (1,13)	5,14 (2,27)	1x	1x

significant when $p < 0,005$ (t-test)
(standard deviation)

Supplemental Experimental Procedures

Phylogenetic reconstruction

We used the protein matrix from [S1], but kept only *P. patens*, *Selaginella moelendorffii* and *Arabidopsis* PIN proteins and the outgroup sequence from *Trichomonas vaginalis* and *Klebsormidium flaccidum*. Phym1 3.0 was used to reconstruct a maximum likelihood tree. ML and NJ bootstrap values were calculated using Phym13.0 and the Phylogeny.fr platform [S2-4].

Auxin transport assays in mesophyll cells from *N. benthamiana*

The coding sequences from the four PpPIN proteins were cloned with stop codon into pDONR221 and subsequently into the gateway destination vector pH2GW7 (for primers, see Suppl. Table 1). This vector was then transformed in the *Agrobacterium* strain C58C1 using electroporation. After agroinfiltration of tobacco leaves, protoplast preparation and transport assays were performed as in [S5]. Relative IAA/NAA export is calculated from effluxed radioactivity as follows: $((\text{radioactivity in the medium at time } t) - (\text{radioactivity in the medium at time } t=0)) * (100\%) / (\text{radioactivity in the medium at } t=0)$.

Root hair assay in *Arabidopsis*

The pDONR221 vectors with the coding sequences including the STOP codon for the four PpPIN proteins were recombined into the gateway destination vector pB7WG2. This vector was used to transform *Arabidopsis*, Columbia ecotype, using the *Agrobacterium* strain C58C1 (Fig. S2B). Transformed plants were selected on BASTA-containing plates (15 mg/l). T3-seedlings were grown vertically in Petri dishes on 0.8% agar 0.5× Murashige and Skoog (MS)

medium containing 1% sucrose, pH 5.9, at 18°C and under a long day light regime. Pictures of the primary root were taken after 8 days of growth with a stereomicroscope.

Cultivation of *P. patens* material

Protonemal tissue was subcultured several times with a minimum of 7 days in between using the ULTRA-TURRAX Tube Drive worksystem (IKA). Subculturing was on cellophane-covered plates with BCD medium [S6], supplemented with 5 mM ammonium tartrate and 0,8% agar. Tissue was grown at 24°C in a long day light regime. Light intensity in the growth chamber is 55 micromoles per m⁻² s⁻¹.

Vector construction

A Gateway multisite destination vector was developed for homologous recombination in *P. patens*. The 108 locus was used as a target of recombination (*Fig. S1A*) [S7]. A fragment of 1005 and 935 bp respectively from the first half (5') and second half (3') of the 108 locus were amplified and cloned in pGEM7ZF (Promega) to generate pL5-L3. A *PmeI* restriction site was included into the primers in order to facilitate removal of the vector backbone from the transgene construct. The Kanamycin marker cassette (nptII coding sequence controlled by a nos promoter and a nos terminator) was cloned between the 108 locus 3' and 5' fragments to obtain pL5-K-L3. A multisite Gateway destination cassette (attR4-ccdB-attR3- Invitrogen) fused at the attR3 region to the CaMV35S terminator was cloned between the 108 locus 5' fragment and the Kanamycin selectable marker to generate a pL5-m34GW7-K-L3 moss destination vector. After recombination, the destination vector is digested with the *PmeI* restriction enzyme and *the linearized DNA was transformed into P. patens protoplasts.*

***P. patens* OE transgenic lines**

The actin promoter from rice was cloned into pDONR P4-P1R [S8] and the coding sequence from AtPIN1 (including stop codon) was cloned into pDONR221 (for primers, see Table S1). All coding sequences from the four *PpPINs* and *AtPIN1* in pDONR221 (including stop codon) were fused together with pACT through two Gateway intermediary vectors (pXb2-m43GW and pDONRP4P3) into the final destination vector (pL5-m43GW7-L3) to generate an overexpression construct (Fig. S1C-D).

Transcriptional fusions with GFP-GUS

A 2kb fragment upstream of the start of each *PpPIN* coding sequence was amplified and was cloned into pDONR P4-P1R (for primers, see Table S1). This was recombined, together with pEN-L1-F-L2 and pEN-R2-S-L3, into pL5-m43GW7-L3 to generate transcriptional reporter lines of each *PpPIN* gene (Fig. S3A).

Translational fusions with GFP

To generate translational fusions to GFP, overlapping PCR using the *PpPIN* genomic fragments and eGFP was used (Fig. S1B, for primers, see Table S1). The fusion fragment was cloned into pDONR221. These vectors were fused to the endogenous *PIN* promoters or to the actin promoter from rice, and recombined into pL5-m43GW7-L3 to generate translational fusions for each PIN protein (Fig. S1C-D, S3A)

Knockout construction

The design for knockout of both *PpPINA* and *PpPINB* is visualised in Figure S1F. A 1000 bp fragment upstream of the start and downstream of the stop were respectively cloned into pDONR P4-P1R and pDONR P2R-P3. The resistance cassettes for nptII from plasmid pMT164 [S6] and for zeocine from pCMAK1 [S9] were cloned into pDONR221 (for primers,

see Table S1). These vectors were then recombined into pXb2-m43GW. The full sequence (homologous recombination sequences and resistance cassette) was then amplified by PCR using iProof (Biorad) and several PCR-reactions were precipitated (for primers, see Table S1). The precipitated DNA was then used to transform *P. patens* protoplasts (Fig. S1E-F). We attempted to generate a triple knockout line, including the long PpPINC, but failed to recover any triple mutant colonies. As the regeneration capacity of the pinapinb mutant lines are reduced compared to wild-type, we believe that triple mutant protoplasts simply cannot regenerate.

***P. patens* phenotyping**

For phenotypic analysis of individual colonies, small pieces of fresh protonemal tissue were inoculated on BCD medium without cellophane and without ammonium tartrate in standard growth conditions. Colonies were photographed every week using a stereomicroscope. For protoplast regeneration, protoplasts were isolated similar to the transformation protocol. After 5 days on regeneration plates, protoplasts were transferred to BCD plates and grown under standard conditions. Pictures were taken with the Axio Imager microscope from Zeiss. To analyse gametophores, gametophores from same-aged colonies were harvested and dissected. Pictures were taken with a stereomicroscope (entire gametophores), or a Leica DMI4000B inverted microscope for close-up pictures of leaves.

GUS Staining and Fluorescence Microscopy

For histochemical staining, tissue was incubated in GUS staining solution [S10] over night at room temperature followed by de-staining in 70% ethanol before microscopic analysis. For fluorescence microscopy, dissected plant material was analyzed using a Leica DMI4000B inverted microscope or a Carl Zeiss LSM710 confocal microscope.

RNA and DNA isolation

Fresh protonemal tissue from *P. patens* and 2-week old seedlings from *Arabidopsis* were snap frozen in liquid nitrogen. Total RNA was extracted with Trizol (LifeTechnologies), followed by purification with RNeasy kit (Qiagen). DNA contaminants were removed using TURBO DNase free-kit (Ambion). Superscript III (Invitrogen) was then used to prepare cDNA. Quantitative RT-PCR was performed on a LightCycler 480 Real-Time PCR System (Roche Diagnostics) with SYBR Green I Master Reagents (Roche Diagnostics) (for qPCR primers, see Table S1).

Supplemental references

- S1. Viaene, T., Delwiche, C.F., Rensing, S.A., Friml, J. (2013). Origin and evolution of PIN auxin transporters in the green lineage. *Trends Plant Sci.* *18*, 5-10.
- S2. Dereeper, A., Guignon, G., Blanc, G., Audic, S., Buffet, S., Chevenet, F., Dufayard, J.F., Guindon, S., Lefort, V., Lescot, M. *et al.* (2008). Phylogeny.fr: robust phylogenetic analysis for the non-specialist. *Nucleic Acids Res.* *36*, 465-469.
- S3. Dereeper, A., Audic, S., Claverie, J.M., Blanc, G. (2010). BLAST-EXPLORER helps you building datasets for phylogenetic analysis. *BMC Evol. Biol.* *11*, 8.
- S4. Guindon, S., Dufayard, J.F., Lefort, V., Anisimova, M., Hordijk, W., Gascuel, O. (2010). New algorithms and methods to estimate maximum-likelihood phylogenies: assessing the performance of PhyML 3.0. *Systematic Biology* *59*, 307-321.
- S5. Henrichs, S., Wang, B., Fukao, Y., Zhu, J., Charrier, L., Bailly, A., Oehring, S.C., Linnert, M., Weiwad, M., Endler, A. *et al.* (2012). Regulation of ABCB1/PGP1-catalysed auxin transport by linker phosphorylation. *EMBO J.* *31*, 2965-80.
- S6. Thelander, M., Nillson, A., Olsson, T., Johansson, M., Girod, P.A., Schaefer, D.G., Zrýd, J.P., Ronne, H. (2007). The moss genes PpSKI1 and PpSKI2 encode nuclear SnRK1 interacting proteins with homologues in vascular plants. *Plant Mol. Biol.* *64*, 559-573.
- S7. Schaefer, D.G., Zrýd, J.P. (1997). Efficient gene targeting in the moss *Physcomitrella patens*. *Plant J.* *11*, 1195-1206.

S8. Proust, H., Hoffmann, B., Xie, X., Yoneyama, K., Schaefer, D.G. (2011). Strigolactones regulate protonema branching and act as a quorum sensing-like signal in the moss *Physcomitrella patens*. *Development* *138*, 1531-1539.

S9. Eklund, D.M., Thelander, M., Landberg, K., Staldal, V., Nilsson, A., Johansson, M., Valsecchi, I., Pederson, E.R., Kowalczyk, M., Ljung, K. *et al.* (2010). Homologues of the *Arabidopsis thaliana* SHI/STY/LRP1 genes control auxin biosynthesis and affect growth and development in the moss *Physcomitrella patens*. *Development* *137*, 1275-84.

S10. Mattsson, J., Ckurshumova, W., Berleth, T. (2003). Auxin signaling in *Arabidopsis* leaf vascular development. *Plant Physiol.* *131*, 1327-1339.